



Cationic pyridyl(benzoazole) ruthenium(II) complexes: Efficient and recyclable catalysts in biphasic hydrogenation of alkenes and alkynes

Aloice O. Ogweno, Stephen O. Ojwach *, Matthew P. Akerman

School of Chemistry and Physics, University of KwaZulu-Natal, Private Bag X01, Scottsville, Pietermaritzburg 3209, South Africa

ARTICLE INFO

Article history:

Received 15 May 2014

Received in revised form 16 July 2014

Accepted 6 August 2014

Available online 22 August 2014

Keywords:

Ruthenium complexes

Structures

Alkenes

Biphasic

Hydrogenation

ABSTRACT

The synthesis, structural characterization of cationic 2-(2-pyridyl)benzoazole)ruthenium(II) complexes and their applications in biphasic hydrogenations of alkenes is reported. Reactions of 2-(2-pyridyl)benzimidazole (**L1**), 2-(2-pyridyl)benzothiazole (**L2**) and 2-(2-pyridyl)benzoxazole (**L3**) with $[\eta^6\text{-(2-phenoxyethanol)}\text{RuCl}_2]_2$ produced the corresponding cationic complexes $[\eta^6\text{-(2-phenoxyethanol)}\text{RuCl}(\mathbf{L1})]\text{Cl}$ (**1**), $[\eta^6\text{-(2-phenoxyethanol)}\text{RuCl}(\mathbf{L2})]\text{Cl}$ (**2**) and $[\eta^6\text{-(2-phenoxyethanol)}\text{RuCl}(\mathbf{L3})]\text{Cl}$ (**3**) in good yields. Solid state structures of **1–3** confirmed the bidentate coordination modes of **L1–L3** and formation of cationic species through displacement of one chloride ligand from Ru(II) coordination sphere. Complexes **1–3** produced active catalysts for high pressure hydrogenation of alkenes both in methanol and biphasic conditions. Relatively lower activities were observed in the hydrogenation of terminal alkynes giving a mixture of alkane and alkene products. Complexes **1–3** were recyclable under biphasic conditions and retained significant catalytic activities in six cycles. Reaction parameters such as substrate/catalyst ratio, temperature, and aqueous/organic ratio affected the catalytic trends.

© 2014 Elsevier B.V. All rights reserved.

1. Introduction

Catalysis is a major player in the manufacturing and processing industries with an estimated 85% of fine and bulk chemicals being produced through heterogeneous or homogeneous processes [1,2]. Homogeneous catalysis is preferred over heterogeneous systems mainly because of high activity, selectivity addition to understanding the mechanisms involved [3–6]. Despite these advantages, homogeneous catalysis is facing several challenges. Most notable are limited catalyst recovery, use of toxic organic solvents and contamination of the products [7–9]. These setbacks have contributed to the limited industrial applications of homogeneous catalysts especially in production of fine chemicals and pharmaceutical products. On the other hand, heterogeneous catalysis offers the possibility for catalyst recovery and recycling, use of less toxic solvents hence greater purity of products [10,11].

While significant progress has been made in developing heterogeneous systems, some drawbacks have been experienced over time. Low catalyst activities, poor selectivity and inability to establish their reaction mechanisms are some of the challenges which have undermined their progress [2]. To overcome these drawbacks

associated with both homogeneous and heterogeneous processes, a new approach of heterogenization of homogeneous systems has emerged. This has been achieved by various methods such as anchoring of single site catalysts on organic or inorganic supports and use of multiphase operations [12,13]. The overall aim of these strategies is to maximize the advantages of both homogeneous and heterogeneous systems, which is to enhance catalyst separation from the reaction mixture while maintaining the selectivity and activity of the catalysts.

Biphasic catalysis, employing water soluble complexes has attracted great attention since its successful industrial application in hydroformylation reactions [14,15]. Thus the design of water-soluble catalysts in other organic transformations such as alkene hydrogenation is significantly gaining momentum [16]. To date, numerous water soluble transition metal based catalysts have been applied in various transition-metal catalyzed reactions [17]. Notable examples include highly efficient and recyclable rhodium catalysts supported on TPPTS ligand (TPPTS = $P(C_6H_{4-m}-SO_3Na)_3$) for the hydrogenation of benzene to cyclohexane [18]. In another related work, Syska et al. reported the use of water-soluble rhodium complexes of carbene ligands in catalytic hydrogenation of acetophenone [19]. More recently, Matsinha et al. described the application of water soluble half-Sandwich Ru(II) – arene complexes in aqueous biphasic hydroformylation of 1-octene [20]. In this paper we report the synthesis, characterization of

* Corresponding author. Tel.: +27 33 260 5239; fax: +27 33 260 5009.

E-mail address: ojwach@ukzn.ac.za (S.O. Ojwach).

cationic η^6 -(2-phenoxyethanol) ruthenium complexes containing 2-(2-pyridyl)benzoazole ligands and their successful application in catalytic hydrogenation of styrene, 1-hexene, 1-octene, 1-decene, 1-hexyne and 1-octyne in methanol. Biphasic catalytic experiments were conducted using water and toluene medium to demonstrate the recyclability of these catalysts. The influence of reactions parameters such as time, substrate/catalyst ratio, temperature, aqueous/organic phase ratio and pressure have been investigated and are herein discussed.

2. Experimental

2.1. Materials and instrumentation

All reactions were carried out under nitrogen atmosphere using a dual vacuum/nitrogen line and standard Schlenk techniques unless stated otherwise. Dichloromethane was distilled from P_2O_5 prior to use. Ru(II) starting material, $[\eta^6\text{-(2-phenoxyethanol)}\text{RuCl}_2]_2$ was prepared according to literature procedure [21,22]. The ligands, 2-(2-pyridyl)benzimidazole (**L1**), 2-(2-pyridyl)bezothiazole (**L2**), 2-(2-pyridyl)bezoxazole (**L3**) were also prepared according to previous methods [23]. NMR spectra were recorded on a Bruker 400 Ultrashield instrument at room temperature in DMSO-d₆ solvent. The ¹H (400 MHz) and ¹³C (100 MHz) chemical shifts are reported in δ (ppm) and referenced to the residual proton in the solvents for ¹H and to solvent signals for ¹³C. Coupling constants (*J*) are measured in Hertz (Hz). Elemental analyses were performed on Thermal Scientific Flash 2000 and mass spectra were recorded on LC Premier micro-mass Spectrometer in the micro-analysis Laboratory at the University of KwaZulu-Natal, South Africa. GC analyses were carried out on Varian CP-3800 GC (ZB-5HT column 30 m × 0.25 mm × 0.10 μm) instrument.

2.2. Syntheses of cationic Ru(II) complexes **1–3**

In a typical synthetic approach, a suspension of $[\eta^6\text{-(2-phenoxyethanol)}\text{RuCl}_2]_2$ (0.10 g, 0.16 mmol) in CH_2Cl_2 (10 mL) was added two molar equivalents of solutions of **L1** (0.06 g, 0.31 mmol) in CH_2Cl_2 (5 mL) and mixture stirred for 24 h at room temperature. After the reaction period, the yellow precipitate formed was filtered, washed with CH_2Cl_2 (15 mL) to obtain compound **1** as a yellow solid. Recrystallization by slow evaporation of the methanol solution of **1** at room temperature afforded single crystals suitable for X-ray analyses. Complexes **2** and **3** were prepared following the same procedure adopted for **1**. All the compounds were characterized by ¹H, ¹³C, mass spectroscopy and microanalyses. The spectral and analytical data obtained are given as supplementary material.

2.3. X-ray crystallography analyses of complexes **1–3**

X-ray data were recorded on a Bruker Apex Duo diffractometer equipped with an Oxford Instruments Cryojet operating at 100(2) K and an Incoatec micro-source operating at 30 W power. The data were collected with Mo $K\alpha$ ($\lambda = 0.71073 \text{ \AA}$) radiation at a crystal-to-detector distance of 50 mm. The data collections were performed using omega and phi scans with exposures taken at 30 W X-ray power and 0.50° frame widths using APEX2 [24]. The data were reduced with the programme SAINT [24] using outlier rejection, scan speed scaling, as well as standard Lorentz and polarization correction factors. A SADABS semi-empirical multi-scan absorption correction [24] was applied to the data. Direct methods, SHELXS-97 [25] and WinGX [26] were used to solve both structures. All non-hydrogen atoms were located in the difference density map and refined anisotropically with SHELXL-97 [23]. All hydrogen atoms were included as idealized contributors in the least squares process.

Their positions were calculated using a standard riding model with C–H_{aromatic} distances of 0.95 Å and $U_{\text{iso}} = 1.2 U_{\text{eq}}$ and C–H_{methylene} distances of 0.99 Å and $U_{\text{iso}} = 1.2 U_{\text{eq}}$. The positions of the hydroxyl O–H of **1** and **3** were constrained using O–H distances of 0.84 Å and $U_{\text{iso}} = 1.5 U_{\text{eq}}$. The hydroxyl O–H of **2**, all hydrogen atoms of the water solvate molecules and the imidazole N–H of **1** were located in the difference density map, and refined isotropically. Disordered solvent molecules were removed from the lattices of **1** and **3**, using Platon SQUEEZE [27]. This leaves solvent accessible voids of 46 and 65 Å³ in the lattices of **1** and **3**, respectively.

2.4. Hydrogenation reactions

2.4.1. Homogeneous experiments

A typical procedure for the catalytic hydrogenation of alkenes was as follows. A Parr High pressure reactor with an in built cooling, heating and stirring systems was charged with styrene (0.56 mL, 5.00 mmol), catalyst (5 mg, 0.01 mmol) and methanol (50 mL) and sealed. It was then evacuated, flushed with H_2 three times and the pressure adjusted to 10 bar. The mixture was stirred at 500 rpm under constant hydrogen pressure for the duration of the reaction period. After the reaction time, the autoclave was vented and samples drawn for GC analyses. The samples were filtered using 0.45 μm micro filters and the solutions analyzed by Varian CP-3800 GC (ZB-5HT column 30 m × 0.25 mm × 0.10 μm). Commercial ethylbenzene was used as an authentic standard to determine the percentage conversion of styrene to ethylbenzene. Percentage conversions were determined by comparing the peak areas of ethylbenzene (product) and styrene substrate.

2.4.2. Biphasic hydrogenation experiments

These reactions were carried in a mixture of water and toluene biphasic system. In a typical experiment, complex **1** (5 mg, 0.01 mmol, equivalent to a substrate/catalyst ratio of 500) was weighed and dissolved in water (25 mL) in a two neck round bottom flask. A solution of styrene 0.56 mL (5.00 mmol) in toluene (25 mL) was added and the mixture transferred to the reactor via canula and sealed. The autoclave was evacuated and flushed with H_2 three times, filled with H_2 and the pressure adjusted to 10 bar and the stirring speed set at 500 rpm. After the reaction period, the reactor was depressurized and the mixture allowed to settle for approximately 5 min. The aqueous layer was then separated from the organic layer using separating funnel. The organic layer was filtered and analyzed by GC to determine the percentage conversion of the substrate to the products. In the recycling experiments, a fresh solution of styrene (0.56 mL, 5.00 mmol) in toluene (25 mL) was added without addition of the catalyst in the aqueous phase. This experiment was repeated for six consecutive cycles.

3. Results and discussion

3.1. Synthesis of cationic ruthenium(II) complexes

Compounds 2-(2-pyridyl)benzimidazole (**L1**), 2-(2-pyridyl)bezothiazole (**L2**) and 2-(2-pyridyl)bezoxazole (**L3**) were synthesized according to literature procedures [23]. Treatment of $[\eta^6\text{-(2-phenoxyethanol)}\text{RuCl}_2]_2$ dimer with two molar equivalents of **L1–L3** in CH_2Cl_2 gave the corresponding monometallic complexes ruthenium(II) $[\eta^6\text{-(2-phenoxyethanol)}\text{RuCl}(\text{L1})]\text{Cl}$ (**1**), $[\eta^6\text{-(2-phenoxyethanol)}\text{RuCl}(\text{L2})]\text{Cl}$ (**2**) and $[\eta^6\text{-(2-phenoxyethanol)}\text{RuCl}(\text{L3})]\text{Cl}$ (**3**) as yellow solids in high yields of 78–88% (Scheme 1). All the complexes were insoluble in chlorinated solvents but were highly soluble in methanol, ethanol and water.

Table 1
Crystal data and structure refinement details for **1**, **2** and **3**.

Crystal data	(1)	(2)	(3)
Chemical formula	C ₂₀ H ₁₉ Cl ₂ N ₃ O ₂ Ru	C ₂₀ H ₁₈ Cl ₂ N ₂ O ₂ RuS·2H ₂ O	C ₂₀ H ₁₈ Cl ₂ N ₂ O ₃ Ru
Molar mass (g mol ⁻¹)	505.35	558.43	506.33
Crystal system, space group	Monoclinic, P2 ₁ /c	Monoclinic, P2 ₁ /n	Monoclinic, P2 ₁ /c
Temperature (K)	100(2)	100(2)	100(2)
a, b, c (Å)	7.1035(5), 26.058(), 11.748(1)	6.6907(4), 26.329(2), 12.2281(6)	7.1859(4), 25.965(2), 11.9779(6)
α, β, γ (°)	α = γ = 90, β = 103.511(3)	α = γ = 90, β = 105.842(2)	α = γ = 90, β = 105.193(2)
V(Å ³)	2114.4(3)	2155.9(2)	2156.71(6)
Z	4	4	4
Radiation type	Mo Kα	Mo Kα	Mo Kα
μ (mm ⁻¹)	1.01	1.10	1.00
Crystal size (mm)	0.39 × 0.15 × 0.10	0.16 × 0.11 × 0.09	0.18 × 0.18 × 0.08
Data collection			
Diffractometer	Bruker Apex Duo CCD diffractometer		
Absorption correction	Multi-scan, SADABS, Bruker 2012		
T _{min} , T _{max}	0.693, 0.905	0.843, 0.907	0.841, 0.925
No. of measured, independent and observed [I > 2σ(I)] reflections	16,799, 3955, 3695	18,423, 4227, 3950	20,146, 4221, 3888
R _{int}	0.025	0.028	0.022
Refinement			
R[F ² > 2σ(F ²)], wR(F ²), S	0.069, 0.157, 1.21	0.026, 0.063, 1.09	0.029, 0.072, 1.03
No. of reflections	3955	4227	4221
No. of parameters	258	291	254
No. of restraints	0	1	2
H-atom treatment	H atoms treated by a mixture of independent and constrained refinement.		
Δρ _{max} , Δρ _{min} (e Å ⁻³)	2.26, -2.22	0.74, -0.48	0.85, -0.80

Complexes **1–3** were characterized by ¹H, ¹³C NMR spectroscopy, micro-analyses, mass spectrometry and single crystal X-ray analyses. As an illustration, ¹H NMR spectrum of **1** showed a broad signal at 15.53 ppm assigned to the N-H proton recorded at 13.07 ppm in the corresponding ligand **L1**. The 6H-pyridyl protons were observed downfield at 9.61, 9.70 and 9.69 ppm in **1**, **2** and **3** respectively in comparison to 8.66 ppm, 8.73 ppm and 8.84 ppm in **L1**, **L2** and **L3** indicating coordination to the ruthenium metal. In general, downfield shifts of the proton signals in **L1–L3** were observed in their corresponding complexes **1–3** (Figs. S1–S7). ESI-MS spectra of **1**, **2** and **3** showed m/z base peaks at 470.02, 486.98 and 471.00 corresponding to the molecular masses of 470.02, 486.98 and 471.00 g mol⁻¹ of the respective cations (Figs. S8–S10). Elemental analyses data of **1–3** were consistent with the proposed structures in **Scheme 1** and confirmed their purity.

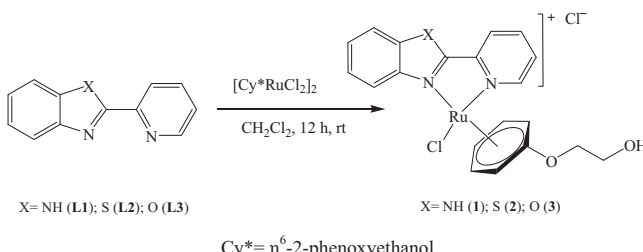
We initially interpreted the ¹H NMR spectra of **1–3** to conform to the change of hapticity of the η⁶-arene group ring from η⁶-η⁴ upon coordination of **L1–L3** to allow for 18-electron systems. Five signals of the η⁶-arene group ring protons were recorded in the ¹H NMR spectra of complexes **1–3** in comparison to three peaks recorded in the Ru starting material (Figs. S1–S3). This indicates that all the protons in the η⁶-arene group ring in **1–3** are unequivalent which is consistent with η⁴-coordination. However, high resolution mass spectral data obtained for **1–3** pointed to the formation of cationic species with the chloride counter anions in the outer sphere. In addition, solid state structures of compounds **1–3** (*vide infra*) confirmed the η⁶-coordination of the η⁶-arene ring. It is thus plausible

to argue that the η⁶-arene ring adopts different coordination modes in solution and solid states.

3.2. Molecular structures of complexes **1–3**

The solid state structures of compounds **1–3** were elucidated using single crystal X-ray crystallography (Fig. 1). While compounds **1** and **3** crystallized in the P2₁/c space group with a single ruthenium cation and associated chloride counter anion in the asymmetric unit (Z = 4), **2** crystallized in the P2₁/n space group as the dihydrate with a single cation and anion as well as two water molecules in the asymmetric unit. The coordination geometry of **1–3** could best be described as a three-legged piano stool. The Ru–Cl bond lengths measures 2.398(2), 2.389(1) and 2.393(1) Å in compounds **1–3**, respectively. A Mogul structural search [28] showed these values to be typical for this class of compounds. The influence of the heteroatom on the Ru–N_{bz} (where N_{bz} is the nitrogen atom of the heterocyclic rings: imidazole, thiazole or oxazole) bond length is evident. Compound **2** with the sulphur atom has the longest Ru–N_{bz} bond length of 2.100(2) Å, while the oxazole complex **3** has the shortest Ru–N_{bz} bond length, 2.078(2) Å. A similar trend is evident when this series of ligands is coordinated to other metal ions, in all cases the M–N_{thiazole} bond length is longer than either the M–N_{imidazole} or M–N_{oxazole} bond length (where M is either Pd(II) or Pt(II)) [29–31]. The Ru–N_{py} bond lengths measure 2.107(5), 2.090(2) and 2.103(2) Å for compounds **1–3**, respectively are statistically similar presumably due to the remote proximity of the heteroatoms to the Ru atom. However, these bond lengths are longer than those previously reported for related Ru(II) complexes of pyridyl ligands, which range from 2.063 to 2.102 Å averaging 2.084 Å [28]. The distances from the centroids of the phenyl rings to the coordinated Ru(II) ions are all statistically comparable for compounds **1–3** ranging from 1.685(2) to 1.696(1) Å (Tables 1 and 2).

The absence of hydrogen bonding in solvent molecules in the lattices of **1** and **3** contributes to the insignificant hydrogen bonding interactions in these structures. Both exhibit similar intermolecular hydrogen bonding between the hydroxyl group of the cation and the chloride counter ion. This interaction, however, does not lead to any extended supramolecular network. The addition of two



Scheme 1. Syntheses of cationic ruthenium(II) complexes **1–3**.

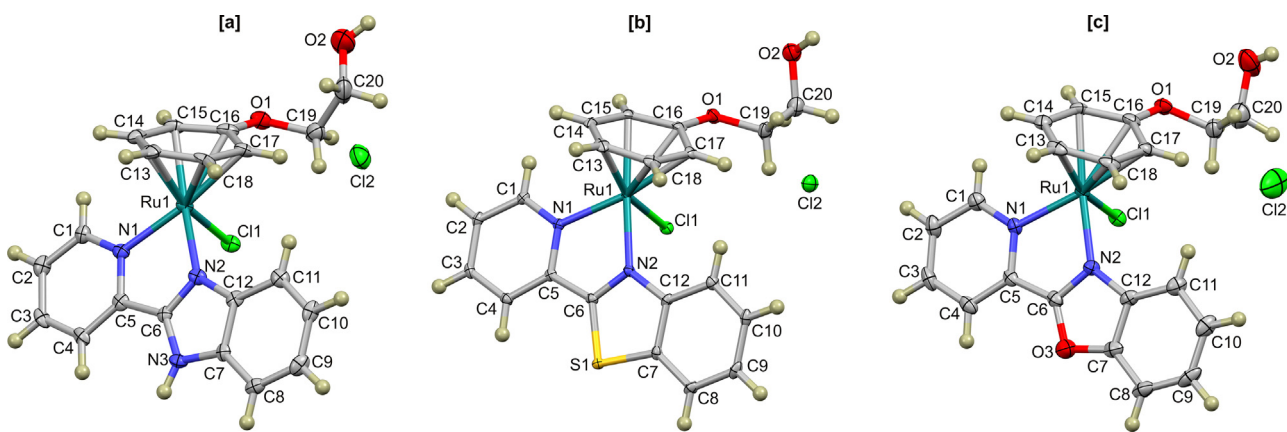


Fig. 1. Thermal ellipsoid plots (50% probability surfaces) showing the atom numbering scheme of **1** (a), **2** (b) and **3**. Hydrogen atoms have been rendered as spheres of arbitrary radius.

water molecules in the lattice of **2** leads to a more complex three-dimensional hydrogen-bonded network. The cations of **2** pack such that there are channels which run co-linear with the *a*-axis. These channels are occupied by water molecules and chloride anions which are linked through extensive hydrogen bonding (Fig. S11). The hydrogen bond lengths and bond angles of **1–3** are summarized in Table S1. The hydrogen bond lengths are all significantly shorter than the sum of the van der Waals radii of the interacting atoms. Although bond distance does not necessarily correlate linearly to bond strength due to packing constraints in the lattice [32], it is likely that these bonds are relatively stronger. The minimal deviation of the hydrogen bond angles from the ideal bond angle, particularly in **2**, further augments this argument.

3.3. High pressure catalytic hydrogenation of olefins

3.3.1. Effect of catalyst structure on hydrogenation of styrene

Preliminary investigations of complexes **1–3** in high pressure catalytic hydrogenation of alkenes were performed using styrene as a model substrate. In a typical reaction, 4.90 mmol of styrene and 0.01 mmol (0.2 mol%, substrate/catalyst ratio of 500) of **1–3** under H₂ pressure (10 bar) in MeOH (50 mL) was employed (Scheme 2). Table 3 contains a summary of hydrogenation data of styrene to ethylbenzene. From Table 3, it is evident that all the complexes

formed efficient catalysts in the homogeneous catalytic hydrogenation of styrene to ethylbenzene giving conversions of 86–100% within 1 h corresponding to TOFs of up to 430 h⁻¹ to 495 h⁻¹.

The identity of the ligand was found to have a profound effect on the catalytic activities of these complexes. For instance, complex **1** bearing the 2-(2-pyridyl)benzoimidazole ligand recorded the highest activity giving conversions of 89% within 0.5 h (TOF = 890 h⁻¹) compared to 42% (TOF = 420 h⁻¹) and 64% (TOF = 640 h⁻¹) for the analogous thiazole and oxazole complexes **2** and **3** respectively. This trend is in good agreement with the acidity trends of **L1–L3**. **L1** is the most acidic while **L2**, containing the S atom, is the least acidic [33]. It is therefore apparent that increased acidity of the ligands plays promoting substrate coordination. A more acidic ligand would therefore increase the electrophilicity of the metal centre and facilitate substrate coordination. This might account for the higher catalytic activities observed in catalyst **1** compared to **2** and **3**. This data agrees with our earlier reports in which the Ru(II) complex of **L1** gave more active catalyst in the transfer hydrogenation of ketones than the corresponding complexes of **L2** and **L3** [34].

3.3.2. Proposed mechanism for hydrogenation of styrene

In order to try and understand the mechanism of hydrogenation reactions catalyzed by complexes **1–3**, we first attempted to establish the homogeneity of the active species. A mercury drop experiment [35] was conducted using complex **1** to establish the homogeneity of the active Ru species or formation of ruthenium colloids/nanoparticles (Table 3, entry 12). Significantly, we did not observe a decrease in the catalytic activity of complex **1** (99%) when five drops of mercury was added to the reaction mixture (Table 3, entries 1 and 12). This confirmed that no heterogeneous ruthenium colloids/nanoparticles were involved and that the hydrogenation reactions were predominantly homogeneous in nature [36,37].

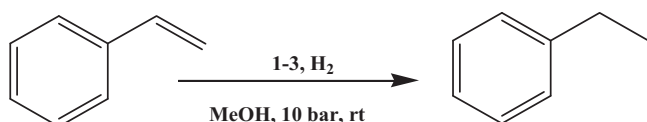
Ruthenium (II)-arene type complexes have been proposed to catalyze the hydrogenation of alkenes through dihydrogen intermediate, since oxidation to Ru(IV) species would be energetically disfavored [38]. Considering that complexes **1–3** are saturated 18-electron systems, a dissociative process would be preferred in order to generate an active dihydrogen intermediate [39]. To allow for substrate coordination, a change of hapticity of the η⁶-arene group ring from η⁶ to η⁴ is most likely since **L1–L3** are expected to be strongly coordination to act as hemi-labile ligands [38]. In addition, the dependence of the hydrogenation reaction on the identity of the ligands (**L1–L3**) implicates their involvement in the catalytic cycles. ¹H NMR spectra of complexes **1–3** (vide supra) further supports this hypotheses, since a change of hapticity of the arene ring was evident (Figs. S1–S3 and S10).

Table 2
Selected bond lengths (Å) and bond angles (°) for **1**, **2** and **3**.

	1	2	3
Bond lengths			
Ru–N _{py}	2.101(5)	2.090(2)	2.103(2)
Ru–N _{bz} ^a	2.088(5)	2.100(2)	2.078(2)
Ru–Cl	2.398(2)	2.389(1)	2.393(1)
Ru–C _p ^b	1.686(2)	1.696(1)	1.690(1)
Bond angles			
N _{py} –Ru–N _{bz}	76.6(2)	76.87(8)	76.61(8)
N _{py} –Ru–Cl	85.2(2)	87.47(6)	84.79(6)
N _{bz} –Ru–Cl	85.3(2)	82.87(6)	85.05(6)

^a Coordinating nitrogen atom of imidazole, thiazole or oxazole heterocyclic rings of **1–3**.

^b Where C_p is the centroid of the coordinating phenyl ring.



Scheme 2. Catalytic hydrogenation of styrene by complexes **1–3**.

Table 3

Effect of reaction parameters on the hydrogenation of styrene to ethylbenzene by **1–3**.

Entry	Catalyst	Cat/Sub	Time (h)	Conversion (%) ^a	Selectivity (%ethylbenzene)	TOF (h ⁻¹) ^d
1	1	500	1	>99(89) ^b	100	495(890)
2	2	500	1	86	100	430
3	3	500	1	90(64) ^b	100	450(640)
4	2	500	1.5	>99	100	330
5	2	500	0.5	42	100	420
6	2	500	0.25	20	100	400
7 ^c	2	200	0.25	>99	100	792
8 ^c	2	500	0.25	49	100	980
9 ^c	2	500	0.5	>99	100	990
10 ^e	3	500	1	32	100	160
11 ^f	3	500	1	29	100	145
12 ^g	1	500	1	99	100	495

^a Conditions: styrene, 4.9 mmol; catalyst; 0.01 mmol (0.2 mol%); 10 bar; MeOH (50 mL), temperature, 30 °C. Determined by GC.

^b Time, 0.5 h.

^c Temperature, 50 °C.

^d TOF in mol substrate mol⁻¹ catalyst h⁻¹.

^e Pressur, bar.

^f Pressure, 1 bar.

^g Mercury drop test (5 drops of mercury added to the reaction mixture).

Starting with complex **1**, we postulate a dissociation of the chloride ligand leading to the formation of dihydrogen intermediate **1a** (**Scheme 3**). Coordination of the substrate is simultaneously accompanied with a change hapticity of the arene group from η^6 - η^4 to give **1b**. Hydride addition to coordinated styrene substrate by dihydrogen ligand leads to the formation of a hydride and alkyl ligands and increase of hapticity from η^4 to η^6 to form ruthenium(IV) intermediate **1c**. Hydride migration in **1c** leads to the formation and elimination of ethylbenzene product and the hydride complex **1d**. Reactions of **1d** with H₂ results in regeneration of the active species **1a** and initiates another catalytic cycle.

3.3.3. Optimization of hydrogenations reaction conditions

Upon establishing that complexes **1–3** form effective catalysts for the hydrogenation of styrene, we turned our attention to the optimization of the reaction conditions. This was accomplished by varying the reaction time, substrate/catalyst ratio, temperature and hydrogen pressure (**Table 3**). From **Table 3**, it is evident that an increase in reaction time resultant in a slight increase in percentage conversions for catalysts **1–3** (**Table 3**, entries 1,3,4,5 and 6). For example, using catalyst **2**, increasing the reaction time from 0.5 h to 1 h was marked by an increase in percentage conversions from 42% to 86% respectively. However, there was a general drop in TOFs of all the catalysts with time. For instance, the TOF of complex **1** dropped from 890 h⁻¹ within 0.5 h to 495 h⁻¹ after 1 h. This trend is consistent with some degree of catalyst degradation with time hence loss of efficiency. It is also worthy to note that complex **2**, containing the benzothiazole ligand **L2**, showed a longer induction period than **1** and **3** (**Table 3**, entries 4 and 6). This feature is likely to originate from the lower electrophilicity of the Ru(II) metal due to the electron rich ligand **L2**. We also observed increased catalytic activities with increase in reaction temperature. Increasing the reaction temperature from 25 °C to 50 °C resulted in an increase in TOF of **2** from 420 h⁻¹ to 990 h⁻¹ respectively (**Table 3**, entries 5 and 9). Similar trends have been reported in literature where Yilmaz et al. observed an increase in TOF from 8 h⁻¹ to 38 h⁻¹ when the reaction temperature was increased from 27 °C to 80 °C [40]. As expected, increasing the hydrogen pressure from 1 bar to 10 bar was also followed by a concurrent increase in TOF of **3** from 145 h⁻¹ to 450 h⁻¹ respectively (**Table 3**, entries 3 and 11).

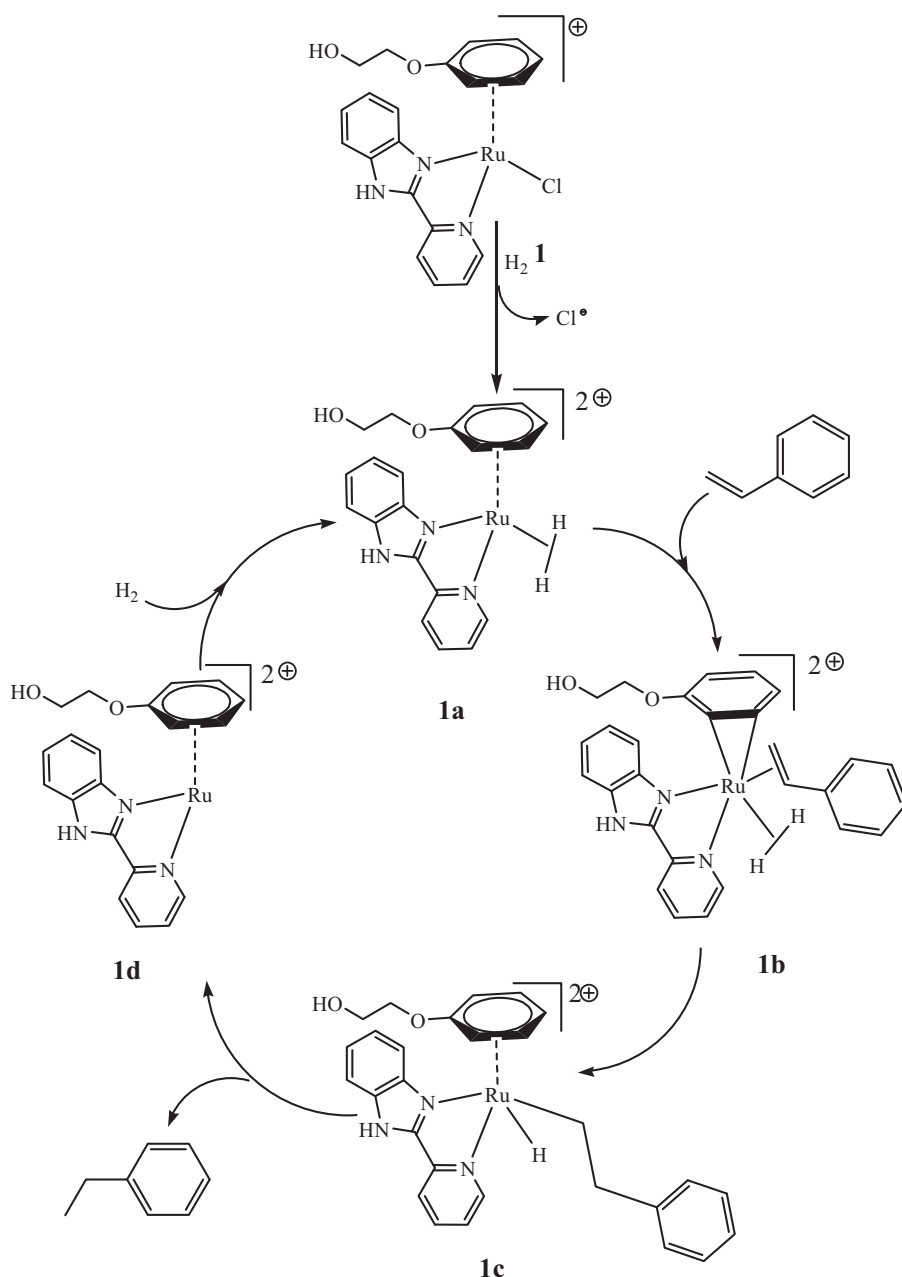
To examine the effect of substrate/catalyst ratio on the hydrogenation of styrene by **2**, we varied the styrene/catalyst ratio from 200 to 500 at room temperature and 10 bar at constant styrene concentration of 5.00 mmol (**Fig. 2**). The conversion of styrene was observed to decrease with increase in substrate to catalyst ratio.

While a 100% conversion was obtained within 15 at 200/1 ratio, only 49% conversion was achieved at higher substrate/catalyst ratio of 500. However, it is important to take cognizance of the higher TOF of 980 h⁻¹ obtained at catalyst/substrate of 500 compared to TOF of 800 h⁻¹ recorded at substrate/catalyst ratio of 200 (**Fig. 2b**). The highest TOF of 1560 h⁻¹ was obtained at substrate/catalyst ratio of 450 (78%). Thus a catalyst/substrate ratio of 450 could be taken as the optimum catalyst loading in the hydrogenation of styrene using complex **2** (**Fig. 2b**).

3.3.4. Substrate scope

Upon optimization of the reactions conditions using styrene as the model substrate, we investigated the versatility of these complexes in catalytic hydrogenation of a range of alkene and alkyl substrates using catalyst **3**. The substrates studied were 1-hexene, 1-octene, 1-decene, 1-hexyne and 1-octyne. The results obtained clearly reflect a significant effect of the substrate identity on the catalytic performance of **3** (**Fig. 3**). Generally higher catalytic activities were reported for alkene substrates compared to the corresponding alkynes. For example, percentage conversions of >99% (TOF = 495 h⁻¹) and 42% (TOF = 210 h⁻¹) were obtained in the hydrogenation of 1-hexene and 1-hexyne respectively (**Fig. 3**). A reasonable explanation for this occurrence could be the stepwise hydrogenation of 1-hexyne to 1-hexene and then to the hexane product. Costa and co-workers reported a similar trend in which the activities of (pyridyl)imine palladium complexes were lower in the hydrogenation of phenylacetylene than in styrene [41].

The selectivities in the hydrogenation of 1-hexyne and 1-octyne were biased towards the corresponding alkanes giving 65% and 52% for hexane and octane respectively (**Fig. 3**). This indicates some degree of catalyst poisoning, which are synonymous with partial hydrogenation of alkynes to the respective alkenes [42]. Increase in chain length of the terminal alkenes from C₁₄ to C₁₈ resulted in a slight drop in percentage conversions of **3** from 99% to 89% respectively, while the activities of observed for C₆–C₁₀ alkenes were comparable. Another interesting observation was the higher catalytic activities of **3** reported in the hydrogenation of unsubstituted alkenes than in styrene reactions. For example, complete conversions of 1-hexene, 1-octene and 1-decene to the corresponding alkanes were realized within 1 h compared to 90% conversion of styrene to ethylbenzene (**Fig. 3**). We attribute these reduced activities in styrene reactions to the π -delocalization of electrons in the phenyl ring, thus reducing the electron density on the double bond. This has the overall effect of limiting styrene substrate coordination to the Ru metal resulting in lower



Scheme 3. Proposed mechanism for the high pressure hydrogenation of styrene by 1.

activities. This trend is consistent with reports by Frediani et al. using $[\text{Ru}(\eta^6\text{-}p\text{-}2\text{-phenoxyethanol})(\text{Cl})(\text{biisoq})](\text{Cl})$ in which they obtained 52.3% (TOF = 85.1 h^{-1}) conversion in the hydrogenation of styrene compared to 99% (TOF = 161.1 h^{-1}) in 1-hexene reactions [43]. In deed, attempts to use complexes **1–3** in the catalytic hydrogenation of benzene to cyclohexane did not result in any activity [44].

The catalytic activities of complexes **1–3** in the homogeneous hydrogenation of alkenes compare favourably with related non-phosphine complexes reported in literature [45]. For example, Ellis et al. reported TOFs of 490 h^{-1} , 76 h^{-1} , 32 h^{-1} and 490 h^{-1} in the hydrogenation of styrene, 1-octene and 1-decene respectively at 60 bar and 60°C using ruthenium cluster complexes $[\text{Ru}_3(\text{CO})_{10}(\text{TPPTN})]$, $[\text{Ru}_3(\text{CO})_9(\text{TPPTN})]$ and $[\text{Ru}_4(\text{CO})_{11}(\text{TPPTN})]$, where TPPTN = tris 3-sulfonatophenyl phosphine trisodium salt [45a]. Comparatively, our ruthenium catalysts displayed TOFs of up to 1560 h^{-1} in these reactions at milder conditions of

10 bar and at room temperature. In another report, Caballero et al. reported TOFs of 1.9 h^{-1} and 32 h^{-1} in styrene and 1-hexene reactions respectively using immobilized $\text{RuCl}_2(\text{bpea})\text{PPh}_3$, ($\text{bpea} = \text{N,N-bis}(2\text{-pyridylmethyl})\text{ethylamine}$) at 5 bar and 50°C [45b].

3.3.5. Biphasic catalysis and catalyst recycling

One of the major challenges hindering industrial applications of homogeneous catalysts is the difficulty in product separation from the reaction mixture in addion to lack of catalyst recycling [5–8]. Various technologies have been employed to improve catalyst recovery and product separation [7]. We thus exploited the water soluble properties of complexes **1–3** to investigate their catalytic activities and recovery in biphasic medium. In a typical experiment, 0.20 mol% (substrate/catalyst ratio = 500) of the complex was dissolved in water (25 mL) to form the aqueous phase and the alkene substrate (5.00 mmol) dissolved in toluene (25 mL)

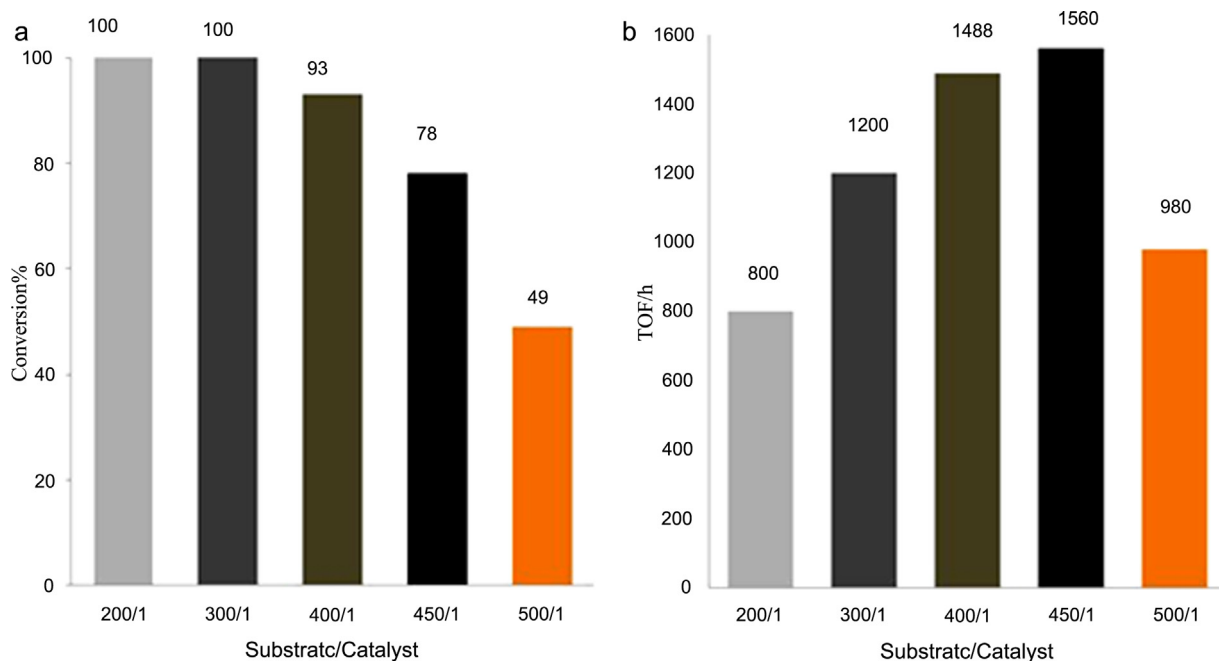


Fig. 2. Effect of substrate/catalyst molar ratio on the activity of **2** on hydrogenation of styrene.

Table 4
Comparison of the TOFs catalysts **1–3** in the first and sixth cycle experiments^a

Entry	Catalyst	H ₂ O/toluene (ml/ml)	TOF ^b h ⁻¹ (Run 1)	TOF ^b h ⁻¹ (Run 6)	% drop	Selectivity (%ethylbenzene)
1	1	1:1	333	203	39	100
2	2	1:1	333	263	21	100
3	3	1:1	333	293	12	100
4	3	2:1	430	320	26	100
5	3	1:2	350	290	17	100
6 ^c	3	1:1	500	400	20	100

^a Conditions: styrene, 4.9 mmol; catalyst; 0.01 mmol (0.2 mol%); 10 bar; temperature, 30 °C; total solvent volume, 50 mL.

^b TOF in mol substrate mol⁻¹ catalyst h⁻¹.

^c Temperature, 50 °C.

to give the organic phase. Catalyst recovery experiments were done by carefully decanting the aqueous phase containing the catalyst followed by addition of an equivalent amount of substrate in toluene without catalyst addition for six cycles (Fig. 4). The catalytic

activities of **1–3** were comparable to the single phase reactions performed in toluene giving complete conversions within 1 h. Most important was the retention of appreciable activities even in the sixth cycle giving conversions of 60%, 79% and 88% for **1**, **2** and **3** respectively (Fig. 4). Table 4 shows the comparative TOF values obtained for complexes **1–3** in the first and sixth runs and corresponding percentage drops in their catalytic activities. Complex **2** achieved 100% conversions in five consecutive runs, translating to a cumulative TON of 2895. These results mirrors those obtained for

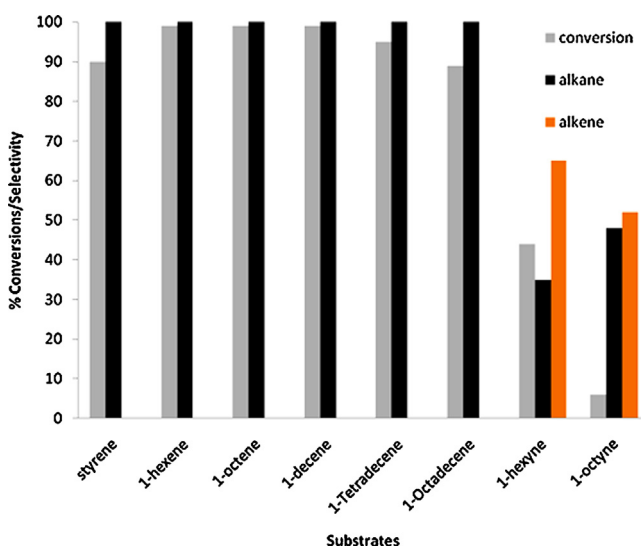


Fig. 3. Catalytic activity and selectivity of complex **3** in the hydrogenation of various substrates. Reaction conditions: substrate, 4.9 mmol; catalyst; 0.01 mmol (0.2 mol%); 10 bar; MeOH (50 mL), temperature, 25 °C; time, 1 h.

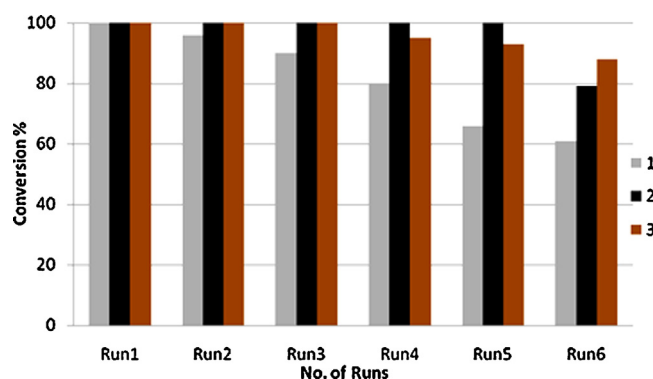


Fig. 4. Conversion of styrene as a function of cycles by **1–3**. Reaction conditions: styrene, 4.9 mmol; catalyst; 0.01 mmol (0.2 mol%); 10 bar; H₂O:Toluene (1:1, total volume, 50 mL), temperature, 25 °C, time, 1 h.

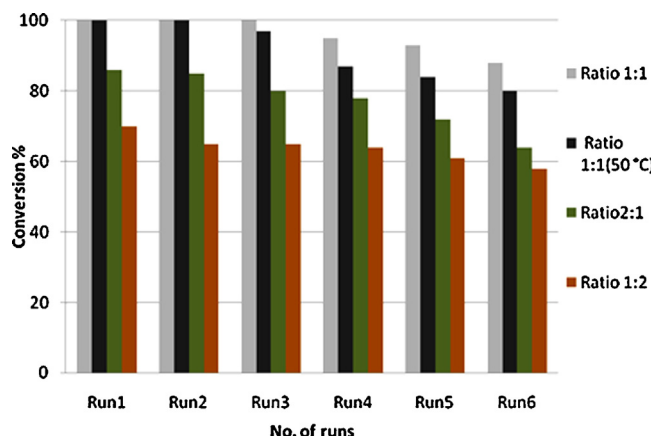


Fig. 5. Influence of aqueous: organic volume ratio and temperature on catalyst regeneration using complex 3.

related single-site water soluble catalysts and heterogeneous systems. For example, using Rh/TPPTS ($\text{TPPS} = [\text{P}(\text{C}_6\text{H}_4-m\text{-SO}_3\text{Na})_3]$), Vangelis and co-workers reported 95% conversion in the hydrogenation of benzene in the fifth cycle [46]. Using heterogeneous palladium nanoparticles supported on polyethylene glycol, Harraz et al. observed 78% conversion of styrene to ethylbenzene in the 10th cycle [18].

Comparatively, complex **1** was the least stable displaying a 39% drop in activity in the sixth run compared to reductions of 21% and 12% reported for **2** and **3** respectively (Table 4, entries 1–3). The low stability of **1** could originate from the weaker donor-ability of the benzimidazole ligand **L1** leading to a relatively unstable complex and is consistent with its observed higher catalytic activity in the homogeneous experiments (Table 3, entries 1–3). This observation demonstrates one of the major challenges in catalyst design of balancing catalyst activity and stability. Another possible reason for reduced catalytic activities in subsequent recycled catalysts could emanate from catalyst leaching into the organic phase, thereby reducing the concentration of the active species in subsequent experiments [17b].

The distribution coefficient of the substrate and catalyst between the solvent systems employed greatly affects catalysts' performance in biphasic reactions [17b]. We investigated the effect of aqueous/organic volume ratios on the biphasic hydrogenation of styrene using catalyst **3**. Fig. 5 and Table 4 provide a summary of the data obtained in the six consecutive runs. The greatest activity was observed using aqueous/organic ratio of 1:1. Increasing the aqueous/organic ratio to 2:1 resulted in a drop of activity from >99% to 86%. A more drastic decline in activity to 70% was observed when higher volumes of the organic phase were employed (aqueous/organic of 1:2). It is therefore conceivable that greater volumes of aqueous phase might limit the diffusion of the catalyst to the interphase. The same argument might apply for the alkene substrate when a large volume of the organic phase is employed. Vangelis et al. [41] reported higher catalytic activities when higher volumes of organic phase was used in the biphasic hydrogenation of benzene. However, in their design, they used neat benzene in the hydrogenation reaction.

Thermal stability is another important feature in catalyst recycling as it leads to catalyst deactivation and loss of activity in subsequent experiments [17c]. The thermal stability of catalyst **3** was studied by comparison of the recycling efficiencies at room temperature and 50 °C (Fig. 5). From the results, it is evident that catalyst **3** exhibited a rapid loss in activity at 50 °C compared to the room temperature reactions. This is demonstrated by a drop of 12% and 20% in the sixth run at room temperature and

50 °C reactions respectively (Table 4, entries, 3 vs 6). It is however, worth noting that catalyst **3** retains significant catalytic activity in the recycling experiments hence these systems can be said to portray some degree of thermal stability.

4. Conclusions

We have successfully isolated and structurally characterized three new cationic (pyridyl)benzoazole ruthenium(II) complexes and extensively studied their applications in homogeneous and biphasic hydrogenation of alkenes and alkynes. Solid state structures of the ruthenium complexes **1–3** support the bidentate coordination mode of the ligands and formation of cationic species with a chloride as a counter anion. All the complexes form highly active catalysts for high pressure hydrogenation of olefins at mild conditions. The electronic contributions of the ligand motif influenced the catalytic activities of the resultant complexes. Higher activities were reported in the hydrogenation of alkenes compared to the corresponding alkynes. The complexes were found to be stable and recyclable in biphasic reactions retaining significant catalytic activities in six consecutive cycles. The aqueous/organic volume ratio and temperature influenced the catalytic activities and recovery of these complexes in biphasic medium. In summary, we have demonstrated a simple synthetic protocol to the design of effective and recoverable water soluble catalysts in biphasic hydrogenation of alkenes.

Acknowledgements

The authors would like to thank University of KwaZulu-Natal and DST-NRF Centre of Excellence in Catalysis (c*change, South Africa) for financial support. We are also grateful to Prof. Gregory Smith (University of Cape Town) for his kind assistance with the ruthenium starting material.

Appendix A. Supplementary data

Supplementary data associated with this article can be found, in the online version, at <http://dx.doi.org/10.1016/j.apcata.2014.08.008>.

References

- [1] B. Cornils, W.A. Herrman, *J. Catal.* 216 (2003) 23–31.
- [2] J. Hagen, *Industrial Catalysis: A Practical Approach*, Wiley-VCH, Weinheim, Germany, 2006, pp. 1–14.
- [3] E.L.V. Goetheer, A.W. Verkerk, L.J.P. van den Broeke, E. de Wolf, B. Deelman, G. van Koten, J.T.F. Keurentjes, *J. Catal.* 219 (2003) 126–133.
- [4] P.G. Jessop, T. Ikariya, R. Noyori, *Chem. Rev.* 99 (1999) 475–493.
- [5] M. Heitbaum, F. Glorius, I. Escher, *Angew. Chem. Int. Ed.* 45 (2006) 4732–4762.
- [6] K. De Smet, S. Aerts, E. Ceulemans, I.F.J. Vankelecom, P.A. Jacobs, *Chem. Commun.* (2001) 597–598.
- [7] I.W. Davies, L. Matty, D.L. Hughes, P.J. Reider, *J. Am. Chem. Soc.* 123 (2001) 10139–10140.
- [8] N. Ren, Y. Yang, Y. Zhang, Q. Wang, Y. Tang, *J. Catal.* 246 (2007) 215–222.
- [9] C. de Bellefon, N. Tanchoux, S. Caravieilhes, *J. Organomet. Chem.* 567 (1998) 143–150.
- [10] S. Alexander, V. Udayakumar, V. Gayathri, *J. Mol. Catal. A: Chem.* 314 (2009) 21–27.
- [11] V. Caballero, F.M. Bautista, J.M. Campelo, D. Luna, R. Luque, J.M. Marinas, A.A. Romero, I. Romero, M. Rodrigues, I. Serrano, J.M. Hidalgo, A. Llobet, *J. Mol. Catal. A: Chem.* 308 (2009) 41–45.
- [12] T.J. Geldbach, P.J. Dyson, *J. Am. Chem. Soc.* 126 (2004) 8114–8115.
- [13] P. Wasserscheid, H. Waffenschimidt, P. Machnitzki, K.W. Kottsieper, O. Stelzer, *Chem. Commun.* 5 (2001) 451.
- [14] C. Stangel, G. Charalambidis, V. Varda, A.G. Coutsolelos, I.D. Kostas, *Eur. J. Inorg. Chem.* (2011) 4709–4716.
- [15] Y. Wang, X. Wu, F. Cheng, Z. Jin, *J. Mol. Catal. A: Chem.* 195 (2003) 133–137.
- [16] B. Cornils, *J. Mol. Catal. A: Chem.* 143 (1999) 1–10.
- [17] (a) P.J. Dyson, D.J. Ellis, T. Welton, *Platinum Met. Rev.* 42 (1998) 135–140; (b) F. Joó, *Aqueous Organometallic Catalysis*, Kluwer Academic Publishers, Dordrecht, Netherlands, 2002; (c) B. Cornils, W.A. Herrmann, *Aqueous-Phase Organometallic Catalysis:*

- Concepts and Applications, 2nd ed., Wiley-Vch Verlag GmbH & Co. KGaA, Weinheim, Germany, 2004.
- [18] F.A. Harraz, S.E. El-Hout, H.M. Killa, I.A. Ibrahim, *J. Catal.* 286 (2012) 184–192.
- [19] H. Syska, W.A. Herrmann, F.E. Kuhn, *J. Organomet. Chem.* 703 (2012) 56–62.
- [20] L.C. Matsinha, P. Malatji, A.T. Hutton, G.A. Venter, S.F. Mapolie, G.S. Smith, *Eur. J. Inorg. Chem.* (2013) 4318–4328.
- [21] J. Soleimannédjad, C. White, *Organometallics* 24 (2005) 2538–2541.
- [22] J. Soleimannédjad, A. Sisson, C. White, *Inorg. Chim. Acta* 352 (2003) 121–128.
- [23] D.W. Hein, R.J. Alheim, J.J. Leavitt, *J. Am. Chem. Soc.* 79 (1957) 427–429.
- [24] Bruker APEX2, SAINT and SADABS, Bruker AXS Inc., Madison, WI, USA, 2012.
- [25] G.M. Sheldrick, *Acta Crystallogr. A* 64 (2008) 112–122.
- [26] L.J. Farrugia, *J. Appl. Crystallogr.* 45 (2012) 849–854.
- [27] A.L. Spek, *Acta Crystallogr. D* 65 (2009) 148–155.
- [28] I.J. Bruno, J.C. Cole, M. Kessler, J. Luo, W.D.S. Motherwell, L.H. Purkiss, B.R. Smith, R. Taylor, R.I. Cooper, S.E. Harris, A.G. Orpen, *J. Chem. Inf. Comput. Sci.* 44 (2004) 2133–2144.
- [29] S. Haneda, Z. Gan, K. Eda, M. Hayashi, *Organometallics* 26 (2007) 6551–6555.
- [30] X.F. He, C.M. Vogels, A. Decken, S.A. Wescott, *Polyhedron* 23 (2004) 155–160.
- [31] J.S. Casas, A. Castineiras, E. Garcia-Martinez, Y. Parajo, M.L. Perez-Paralle, A. Sanchez-Gonzalez, J. Sordo, Z. Anorg. Allg. Chem. 631 (2005) 2258–2264.
- [32] T. Steiner, *Chem. Commun.* 8 (1997) 727–734.
- [33] J.M. Abboud, C. Roussel, E. Gentric, K. Sraidi, J. Lauransan, G. Guiheneuf, M.J. Kamlet, R.W. Taft, *J. Org. Chem.* 53 (1988) 1545–1550.
- [34] A.O. Ogweno, S.O. Ojwach, M.P. Akerman, *Dalton Trans.* 43 (2014) 1228–1237.
- [35] P. Foley, R. DiCosimo, G.M. Whitesides, *J. Am. Chem. Soc.* 102 (1980) 6713–6725.
- [36] O. Prakash, K.N. Sharma, H. Joshi, P.L. Gupta, A.K. Singh, *Organometallics* 33 (2014) 2535–2543.
- [37] (a) Y. Lin, R.G. Finke, *Inorg. Chem.* 33 (1994) 4891–4910;
 (b) R. Crabtree, D.R. Anton, *Organometallics* 2 (1983) 855–859.
- [38] C. Daguenet, R. Scopelliti, P.J. Dyson, *Organometallics* 23 (2004) 4849–4857.
- [39] A. Grabulosa, A. Mannu, A. Mezzetti, G. Muller, *J. Organomet. Chem.* 696 (2012) 4221.
- [40] F. Yilmaz, A. Mutlu, H. Unver, M. Kurtca, I. Kani, *J. Supercrit. Fluids* 54 (2010) 202–209.
- [41] M. Costa, P. Pelagatti, C. Pelizzi, D. Rogolino, *J. Mol. Catal. A: Chem.* 178 (2002) 21–26.
- [42] (a) H. Lindlar, R. Dubuis, *Org. Synth. Coll.* 50 (1973) 880;
 (b) L.E. Overman, M.J. Brown, S.F. McCann, *Org. Synth. Coll.* 8 (1993) 609;
 (c) M. Garacia-Mota, J. Gomez-Diaz, G. Novell-Leruth, C. Vargas-Fuentes, L. Bel-larosa, B. Bridier, J. Perez-Ramirez, N. Lopez, *Theor. Chem. Acc.* 128 (2010) 663–673.
- [43] P. Frediani, C. Giannelli, A. Salvini, S. Ianelli, *J. Organomet. Chem.* 667 (2003) 197–208.
- [44] Complex **3** (5 mg, 0.01 mmol) in methanol (50 mL) and benzene (0.44 mL, 4.9 mmol) H₂ pressure, 10 bar, time 1 h. No catalytic activity was observed.
- [45] (a) D.J. Ellis, P.J. Dyson, D.G. Parker, T. Welton, *J. Mol. Catal. A: Chem.* 150 (1999) 71–75;
 (b) V. Caballero, F.M. Bautista, J.M. Campelo, D. Luna, R. Luque, J.M. Marinas, A.A. Romero, I. Romero, M. Rodriguez, I. Serrano, J.M. Hidalgo, A. Llobet, *J. Mol. Catal. A: Chem.* 308 (2009) 41–45;
 V.J. Catalano, T.J. Craig, *Polyhedron* 19 (2000) 475–485;
 (b) C. Aliende, M.P. Manrique, F.A. Jalon, B.R. Manzano, A.M. Rodriguez, G. Espino, *Organometallics* 31 (2012) 6106–6123;
 (c) M. Heckenroth, V. Khlebnikov, A. Neels, P. Schertenberger, M. Albrecht, *Chem-CatChem* 3 (2011) 167–173.
- [46] C. Vangelis, A. Bouriazos, S. Sotiriou, M. Samorski, B. Gutsche, G. Papadogianakis, *J. Catal.* 274 (2010) 21–28.